

19. September 2014

Analysis of shower shapes of pions and protons from the tungsten analogue hadronic calorimeter

A. Burger^{*†}

^{} CERN, Switzerland, [†] Ludwig-Maximilians-Universitaet Muenchen, Germany*

Abstract

In this report, analysis results of test-beam data taken with the CALICE tungsten analogue hadronic calorimeter prototype are presented. Proton and pion-induced showers originating from a particle beam of an momentum range of 25-150 GeV are examined. As a first part of the study, a comparison between data and two GEANT4 Monte-Carlo simulations with regard to variables describing hadronic shower fluctuations is performed. In the second part of this report, the separation potential of the W-AHCAL for protons and pions is discussed.

Contents

1	Introduction	3
2	The testbeam measurements	3
2.1	The CALICE tungsten scintillator hadronic calorimeter	3
2.2	Test-beam measurement with the W-AHCAL prototype	3
2.3	Data selection	4
2.4	Monte-Carlo models	4
3	Fluctuation of hadronic showers	4
3.1	Fluctuations of the longitudinal shower development	4
3.2	Fluctuations of the longitudinal shower depth	5
4	Proton and Pion distinction using a Boosted decision tree	8
4.1	Method	8
4.2	Shower characteristics used for the distinction	8
4.3	Results	9
5	Conclusion and Outlook	10
6	Acknowledgements	11

1 Introduction

The tungsten analogue hadronic calorimeter (W-AHCAL) is a prototype of a hadronic sampling calorimeter for CLIC, a concept of a future e^+e^- collider with a centre-of-mass energy in the multi-TeV range. A test-beam experiment with this prototype was performed at the CERN SPS in summer and autumn 2011 [1]. The intention of the test-beam experiment with the CALICE scintillator tungsten hadronic calorimeter is to study the performance of the detector concept in realistic conditions, its response to different kind of particles, validate Monte-Carlo simulation models and to plan for the next step of detector development for an optimized detector. The first part of this project consists of a comparison between Monte-Carlo simulations and test-beam data. Here, the goodness of description of variables describing the fluctuations of hadronic showers is investigated. As a second part of the project, the potential to separate protons and pions only using information of the calorimeter is tested.

2 The testbeam measurements

This section provides an overview of the CALICE W-AHCAL test-beam experiment as performed in 2011 at the CERN SPS and the corresponding Monte-Carlo models.

2.1 The CALICE tungsten scintillator hadronic calorimeter

The CALICE scintillator tungsten HCAL is one of the prototypes of high granularity calorimeters designed and tested by the CALICE collaboration for future collider experiments.

This prototype consists of a stack of 38 sampling layers where tungsten is used as absorber and scintillator tiles as detector material. The calorimeter depth corresponds to 4.9 hadronic interaction lengths (λ_i). The readout is done with Silicium Photomultipliers (SiPM). For more detailed information on the W-AHCAL see [2].

2.2 Test-beam measurement with the W-AHCAL prototype

The test-beam measurement was performed at the CERN SPS (Super-Proton-Synchrotron). The set-up of the measurement is illustrated in figure 1.

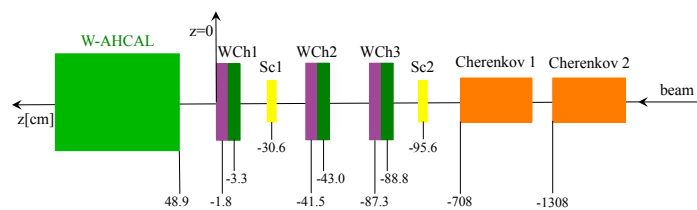


Figure 1: Schematic set-up of the test-beam experiment on the W-AHCAL prototype. For explanations, see text.

The W-AHCAL prototype can be seen at the very left in figure 1. In order to determine the particle type in the measurement, the beam, coming from the right, first passes two Cherenkov counters (Cherenkov1 and Cherenkov2). For triggering, scintillators (SC1 and SC2) are used and a position measurement is done with delay wire chambers (WCh1-3).

Data were taken with electron, muon and mixed hadron beams with an energies range from 10-300 GeV. Energy calibration was done using muons, all energy units in this report are therefore in MIPs [3].

2.3 Data selection

A number of selection cuts is applied on the event sample: Particles are identified with the information provided by the Cherenkov detectors (see section 2.2, figure 1). Muon contamination from in-flight decay of hadrons is reduced by requiring certain track and cluster properties which can be measured with information of the high-granularity calorimeter. Furthermore, electron-like and empty events are rejected. More details on the selection cuts are given in [3].

2.4 Monte-Carlo models

The detector with the W-AHCAL concept described in section 2.1 and the experimental set-up as shown in figure 1 is implemented in a GEANT 4 based application called Mokka, version 9.6.p01. For this study, two physics lists are used for the Monte-Carlo simulations: QGSP_BERT_HP and FTFP_BERT_HP. For more information on the Monte-Carlo models see [3].

3 Fluctuation of hadronic showers

This section discusses the question whether the Monte-Carlo simulations provide a sufficiently good description of the data of the test-beam measurement. As a method to investigate this, shower properties are compared between data and Monte-Carlo. Similar studies have already been done in [1]. This report specializes on the fluctuations of hadronic showers.

3.1 Fluctuations of the longitudinal shower development

As a first step, the fluctuations with respect to the energy deposition in longitudinal direction is investigated. Figure 2 shows the distribution of the energy deposition in the calorimeter layers with respect to the shower start for pions with a beam energy of 80 GeV. Overlaid is a profile histogram visualizing the mean value of energy deposition and its standard deviation.

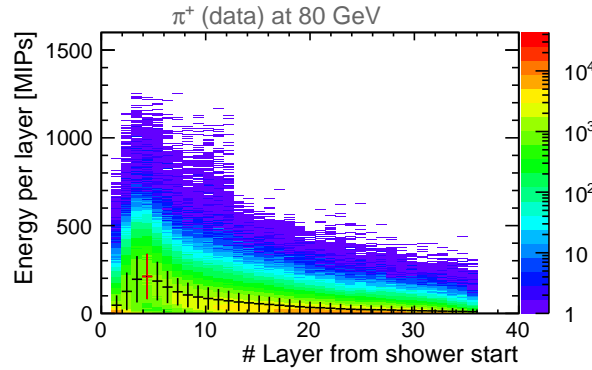


Figure 2: Energy deposit in each calorimeter layer for pions at 80 GeV. The profile histogram visualizes the mean and the standard deviation of the distribution.

The energy spread per layer shows that the energy deposition fluctuates. The size of the error bars of the profile histogram shown in figure 5 corresponds to one standard deviation in positive and negative direction. Representatively, the spread at the layer with the maximum energy deposition (highlighted red in figure 2) is studied as a function of the beam energy in figure 3. Also the spread with respect to two other layers was examined but this would go beyond the scope of this summer student report.

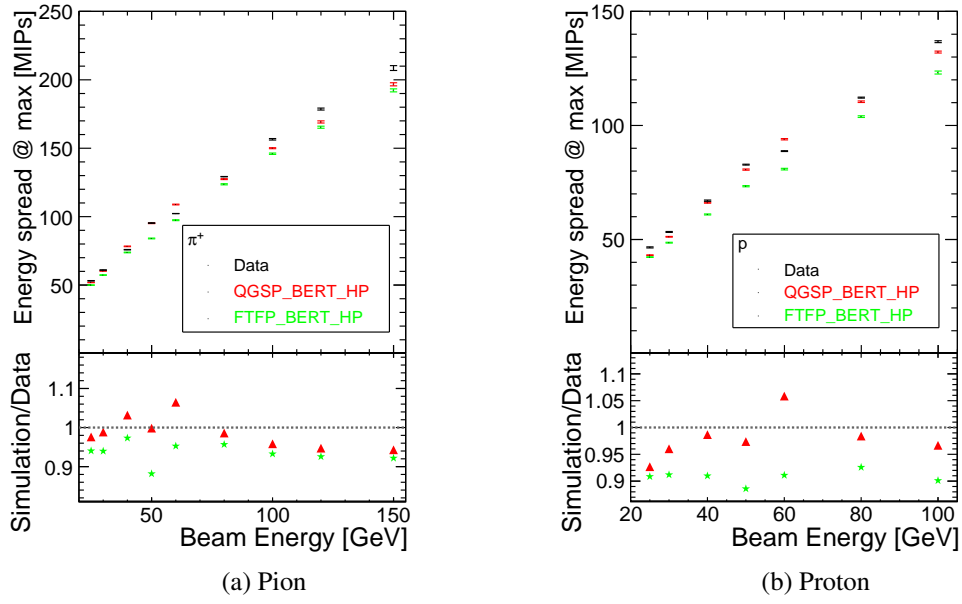


Figure 3: Spread of the energy deposition at the mean layer of maximum energy deposition as a function of the beam energy for pions (a) and protons (b).

The Monte-Carlo samples mostly underestimate this spread in case of protons and pions by up to 10%. The QGSP_BERT_HP model shows a better agreement with data than the FTFP_BERT_HP model.

3.2 Fluctuations of the longitudinal shower depth

This subsection focuses on the shower depth in longitudinal direction, its fluctuation, and the agreement between data and Monte-Carlo with respect to these quantities. Here, the study of the shower depth at 67% of the full shower energy is presented. The quantity gives information about how many layers it takes to absorb 67% of the full shower energy. For illustration, the distribution of the longitudinal shower depth at 67% of pions for a beam energy of 80 GeV is shown in figure 4.

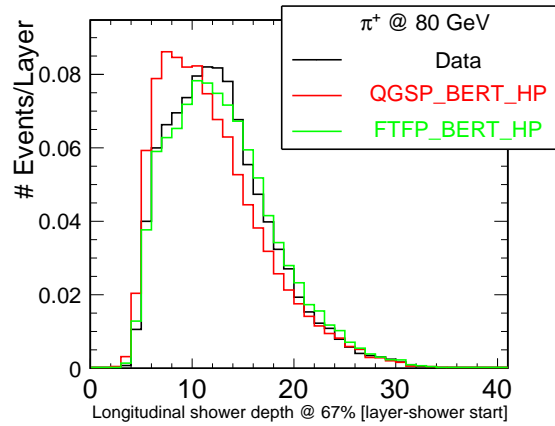


Figure 4: Distribution of the longitudinal shower depth for pions with a beam energy of 80 GeV.

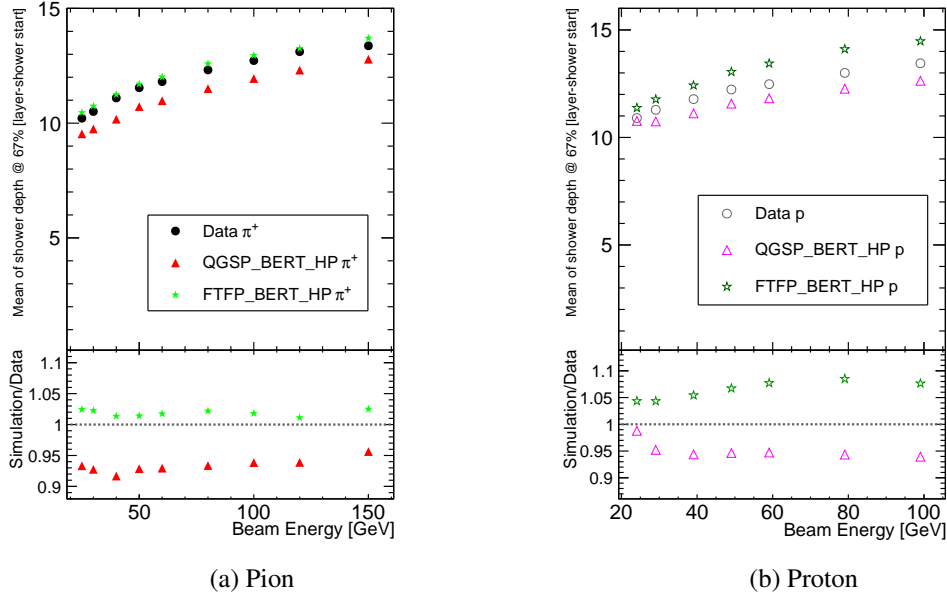


Figure 5: Mean of longitudinal shower depth at 67% of the full shower energy as a function of the beam energy for pions (a) and protons (b).

Figure 5 shows the mean value of the shower depth for protons and pions for data and the two Monte-Carlo models. Both Monte-Carlo models are in good agreement with data whereas FTFP_BERT_HP is better for pions and QGSP_BERT_HP is better for protons. In these cases, an agreement of better than 5% is archived. For the other Monte-Carlo, respectively, an agreement with data of within 10% is observed.

Proton showers are deeper than pion showers on average (see figure 7a). Inelastic collisions of the π^+ with the absorber material tend to result in more π^0 which decay to photons than proton-induced showers. Therefore, π -showers have a larger electromagnetic shower component which are more compact than hadronic showers.

The spread of the mean longitudinal shower depth is shown in figure 11. Data and MC are in an agreement within 5%. Proton and Pion comparison is presented in figure 12, panel (b). The spread is larger for pions despite of the lower mean.

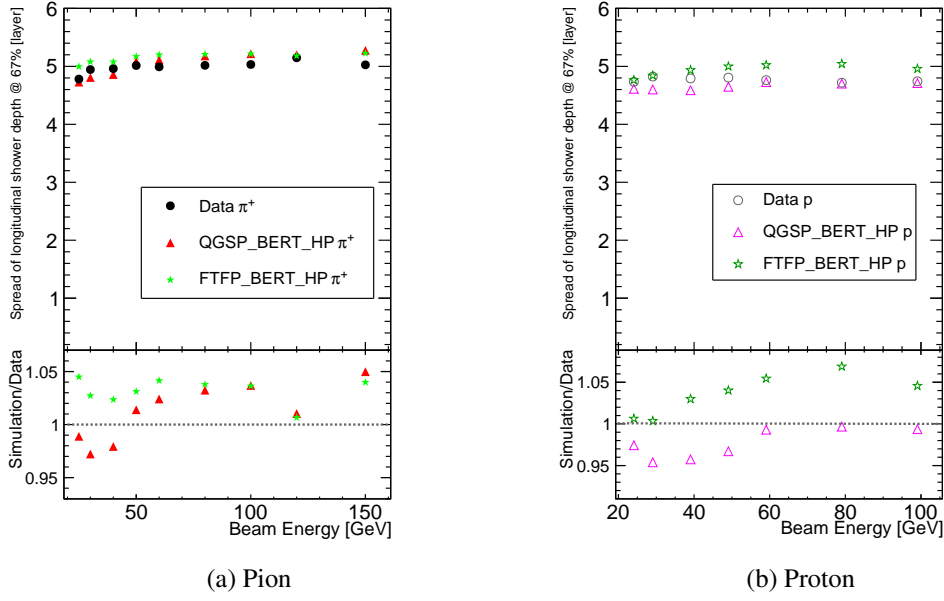


Figure 6: Spread of longitudinal shower depth at 67% of the full shower energy as a function of the beam energy for pions (a) and protons (b).

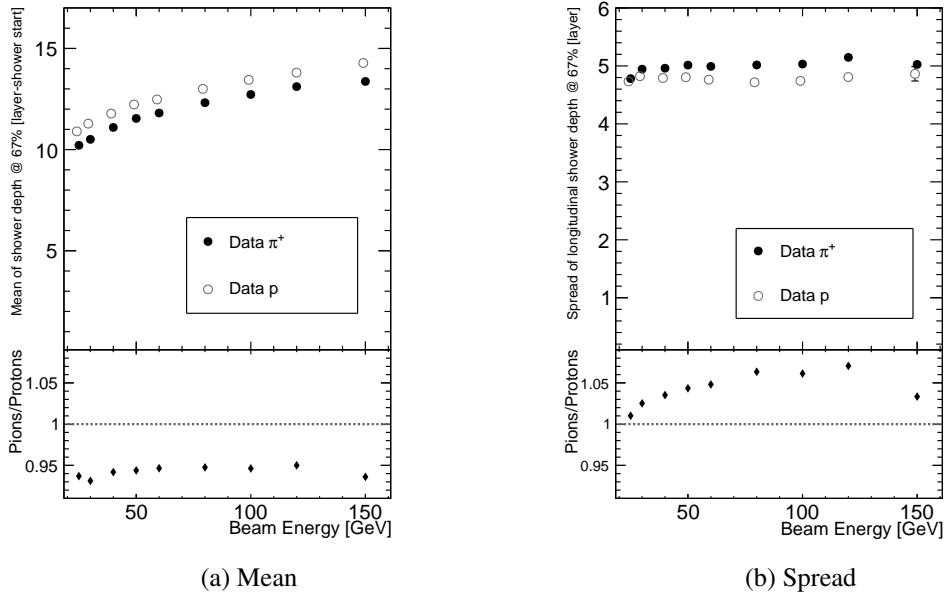


Figure 7: Comparing pions (a) and protons (b) with respect to the mean and the spread of the longitudinal shower depth at 67% of the full shower energy.

Analogue to the fluctuation of the longitudinal shower development and depth, the shower fluctuations in the radial direction and the radial shower width were also investigated. Furthermore, studies were carried out concerning the longitudinal shower depth at 33% of the full shower energy. But this would go beyond the scope of this Summer Student project report.

4 Proton and Pion distinction using a Boosted decision tree

Some differences between proton and pion showers in the W-AHCAL have already been discussed in section 3.2, like for instance, that proton showers are deeper in the HCAL than pion showers (see figure 7). In the following, the possibility is tested whether protons and pions can be distinguished only using the information provided by the HCAL. The distinction is done on the base of shower characteristics.

4.1 Method

A boosted decision tree (BDT), a machine learning tool to classify events in a sample, is used as a tool for this task. The BDT is implemented in TMVA (Toolkit for Multivariant Analysis). More information on the Boosted Decision Tree method and TMVA can be found in [4] and [5].

4.2 Shower characteristics used for the distinction

The separation potential is evaluated using 30 variables describing the shower characteristics. The distinction is not expected to be easy as proton- and pion-induced showers look very similar. Therefore, a lot of variables are included in the BDT and tested whether they will turn out to be useful or not. Whether a variable is important depends on how different this variable is for protons and for pions. The separation potential is first tested using the QGSP_BERT_HP Monte-Carlo as training and testing sample, then tried on data, whereas data are also used for testing and training.

Here, two examples of variables implemented in the BDT are given:

In section 3.2, protons and pions were already compared with respect to their longitudinal shower depth. Figure 8 shows the distribution of the longitudinal shower depth at 67% of the full shower energy for a beam energy of 60 GeV. Figure 8 is in fact in accordance with the observation made in section 3.2 that proton showers are deeper than pion showers. But the difference is not very striking, especially in data (see figure 8b). The difference between protons and pions seems to be in fact slightly larger in Monte-Carlo than in data.

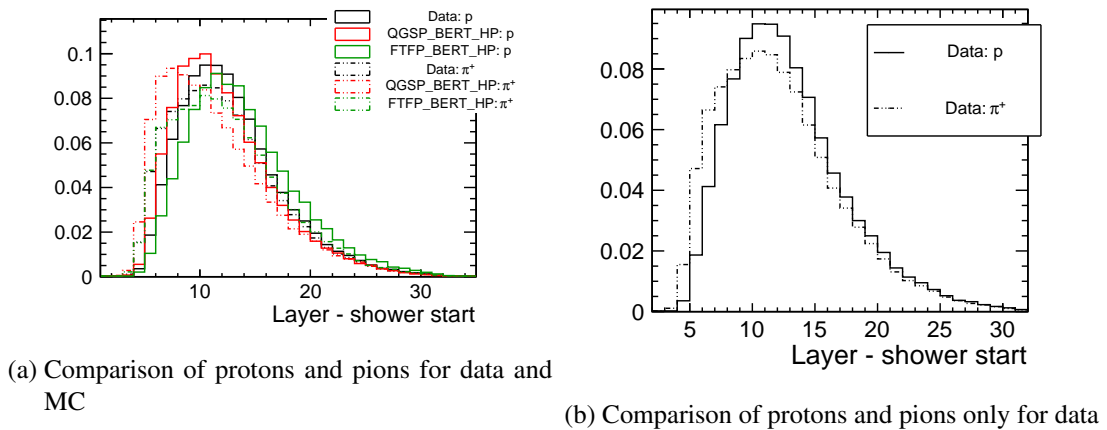
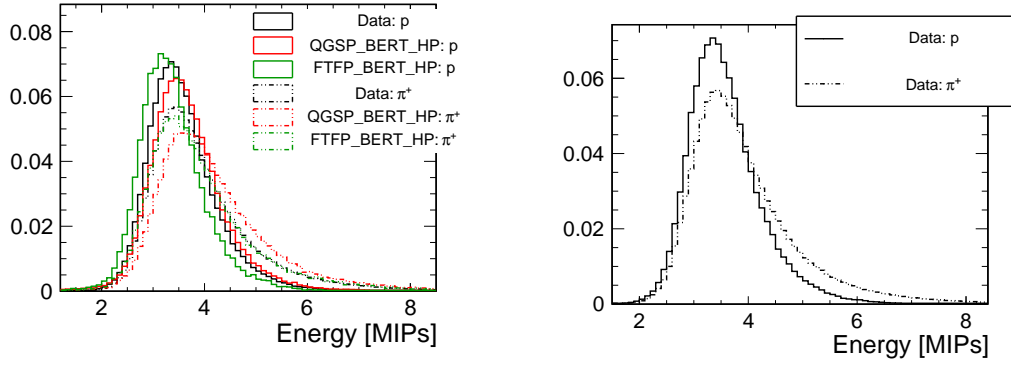


Figure 8: Distribution of the longitudinal shower depth at 67% of the full shower energy.

The same conclusion can be drawn when having a look at the mean hit energy normalized to a 3×3 cm²-cell (see figure 9). This variable will be one of the most important variables and will have a large impact in the separation.

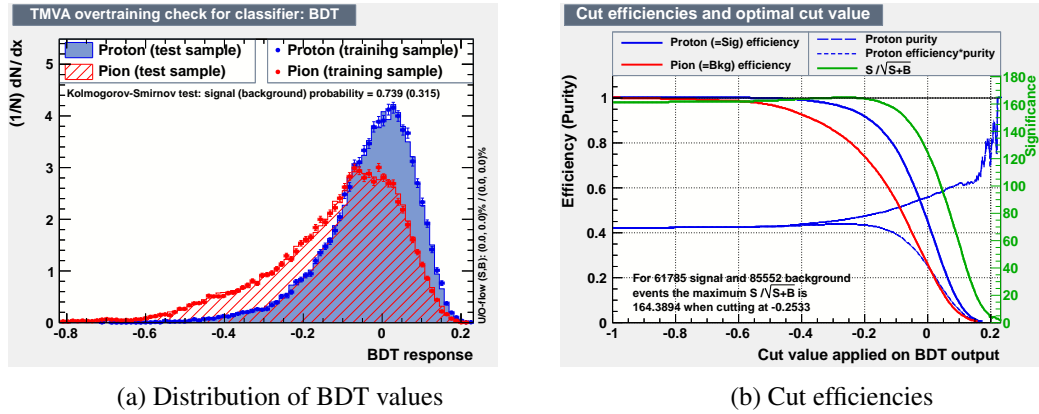


(a) Comparison of protons and pions for data and MC. (b) Comparison of proton and pions only for data.

Figure 9: Mean hit energy per cell, normalized to a $3 \times 3 \text{ cm}^2$ cell.

4.3 Results

The separation is applied by implementing a cut on the BDT values which were assigned to each event based on whether the event is more proton- or pion-like (see [4]). Rejecting all events with BDT values below this proposed cut, a maximum significance of the sample is archived. The significance ($S = \frac{N_{\text{Proton}}}{\sqrt{N_{\text{Proton}} + N_{\text{Pion}}}}$, whereas N is the number of events) is the optimal trade-off between a high sample purity and a high remaining event number. Figure 10a shows the distribution of BDT values when using QGSP_BERT_HP for training and for testing.



(a) Distribution of BDT values

(b) Cut efficiencies

Figure 10: BDT results for the case of QGSP_BERT_HP training and testing. Panel (a) shows the BDT values distribution and panel (b) the cut efficiencies.

Figure 10 makes it evident that the shower properties of protons and pions are very similar as their corresponding BDT value distributions overlap very strongly. After applying the optimal cut on the BDT value, the sample still will be contaminated. This optimal cut can be extracted from figure 10b. The highest significance is archived with a BDT cut of -0.2533.

Applying this cut, 95% of the protons and 80% of the pions are kept. That means, that it is possible to accumulate protons or pions in a sample but it is not possible to really separate them.

The BDT separation method is now applied on the test-beam sample, whereas data is used for training and testing. The distributions of the BDT values for protons and pions in figure 11a largely coincide and estimating qualitative, the overlap between protons and pions is greater than in the Monte-Carlo study. This is underlined by the cut efficiency plot in figure 11b: the proton efficiency for a cut value at -0.4951 is given by 97% while keeping 87% of the pions. The best significance is therefore slightly lower than in case of Monte-Carlo testing and training.

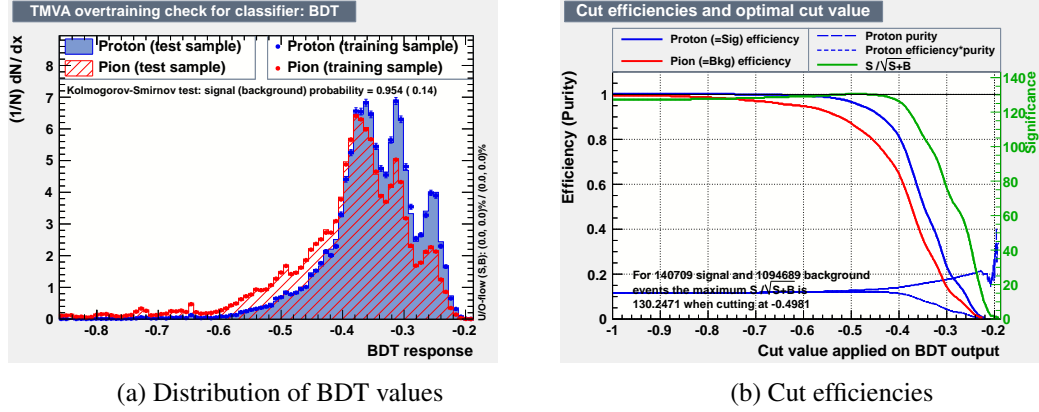


Figure 11: BDT results for the case test-beam data used for training and testing. Panel (a) shows the BDT values distribution and panel (b) the cut efficiencies.

Hence, it is a little bit more difficult to separate protons and pions and for data, the separation is not so well applicable than predicted in Monte-Carlo.

The main reason for this overestimation is the yet existing discrepancy between data and Monte-Carlo but another effect playing a role could issue from contamination of the test-beam data of other particle types. For instance, there could be pions or kaons in a proton test-beam data sample whereas the Monte-Carlo samples consist purely of protons [6].

Protons and pions are different with respect to the available energy $E_{\text{available}}$ in the detector. This arises from the fact that the pion decays into two much lighter particles transforming most of its rest energy into shower energy whereas the protons is stable. Variables containing information about energy deposit are affected by this effect and their distributions are therefore expected to be shifted to lower energies in case of protons. The impact of this effect has been checked doing BDT separation studies with QGSP_BERT_HP proton and pion samples with the same $E_{\text{available}}$. Also with proton and pion samples at the same $E_{\text{available}}$ it is still possible to accumulate one particle type with the presented method. However, the separation potential is slightly reduced.

5 Conclusion and Outlook

The agreement between data and Monte-Carlo with respect to variables describing hadronic shower fluctuation in longitudinal and radial direction and fluctuations of the shower depth is of the order of 5-15%. A general tendency is not observed, none of the two Monte-Carlo models is generally better. Which model provides a better description is different for each variable and sometimes also dependent on the particle type.

As expected, a complete separation between protons and pions in the hadronic calorimeter is not possible, their shower properties and shape are too similar. But nevertheless, some small differences between proton and pion showers allow to accumulate one particle type in a sample. These differences cannot

be explained by the slight difference of available energy in the detector when using pions and protons at the same beam energy. The Monte-Carlo simulation overestimates the difference between protons and pions slightly compared to data. A possible reason might be a contamination of the test-beam data sample with another particle type. As a next step, one could check this by admixing contamination to the Monte-Carlo sample and to repeat the study for this new sample.

6 Acknowledgements

I would like to thank my supervisors Eva Sicking and Dominik Dannheim for their competent support and kind help during this Summer Student project. I learned very much in this project and enjoyed working with you very much! Thank you very much for helping me whenever I had problems or questions and for your patience doing so!

Thanks also to the group for their warm welcome. I very much appreciated the nice working atmosphere in the group.

References

- [1] A. Lucacu-Timoce, *Shower development of particles with momenta from 10 to 100 GeV in the CALICE Scintillator-Tungsten HCAL* (2013).
- [2] L. Linssen et al., eds., *CLIC Conceptual Design Report: Physics and Detectors at CLIC*, CERN-2012-003, CERN, 2012, arXiv: [1202.5940 \[physics.ins-det\]](#).
- [3] C. Adloff et al., *Shower development of particles with momenta from 1 to 10 GeV in the CALICE Scintillator-Tungsten HCAL*, JINST **9** (2014) P01004, DOI: [10.1088/1748-0221/9/01/P01004](#), arXiv: [1311.3505 \[physics.ins-det\]](#).
- [4] A. Hocker et al., *TMVA Executive Summary*, 2014, URL: http://tmva.sourceforge.net/#exec_summary.
- [5] A. Hocker et al., *TMVA - Toolkit for Multivariate Data Analysis*, PoS **ACAT** (2007) 040, arXiv: [physics/0703039 \[PHYSICS\]](#).
- [6] D. Dannheim et al., CERN Linear Collider Detector collaboration, *Particle Identification with Cherenkov detectors in the 2011 CALICE Tungsten Analog Hadronic Calorimeter Test Beam at the CERN SPS* (2013).